Noncoherent Adaptive Channel Identification Algorithms for Noncoherent Sequence Estimation

Robert Schober, *Student Member*, IEEE, and Wolfgang H. Gerstacker, *Member*, IEEE

Abstract

In this letter, two novel noncoherent adaptive algorithms for channel identification are introduced. The proposed noncoherent least–mean–square (NLMS) and noncoherent recursive least–squares (NRLS) algorithms can be combined easily with noncoherent sequence estimation (NSE) for M–ary differential phase–shift keying (MDPSK) signals transmitted over intersymbol interference (ISI) channels. It is shown that the resulting adaptive noncoherent receivers are very robust against carrier phase variations. For zero frequency offset the convergence speed and the steady–state error of the noncoherent adaptive algorithms are similar to those of conventional LMS and RLS algorithms. However, the conventional algorithms diverge even for relatively small frequency offsets, whereas the proposed noncoherent algorithms converge for relatively large frequency offsets. Simulations confirm the good performance of NSE combined with noncoherent adaptive channel estimation in time–variant (fading) ISI channels.

Index Terms:

Noncoherent adaptive channel identification/estimation, noncoherent least–mean–square (NLMS) algorithm, noncoherent recursive least–squares (NRLS) algorithm, noncoherent sequence estimation (NSE), intersymbol interference (ISI) channels.

1 Introduction

In many existing communication systems (e.g., Global System for Mobile Communication (GSM), United States Digital Cellular (IS–54, IS–136)) coherent maximum–likelihood sequence estimation (MLSE) [1, 2] is used for equalization of intersymbol interference (ISI) channels. MLSE requires knowledge of the possibly time–variant channel impulse response and therefore, adaptive channel identification algorithms have to be employed. In practice, least–mean–square (LMS) and recursive least–squares (RLS) algorithms are preferred for this purpose [3, 4, 5, 6, 7, 8].

Recently, noncoherent sequence estimation (NSE) schemes for ISI channels have been proposed [9, 10, 11, 12, 13]. Although, in principle, NSE is also applicable to multi–amplitude signals [11], for simplicity, in this letter we restrict ourselves to M–ary differential phase–shift keying (MDPSK) signals. In contrast to coherent sequence estimation, NSE does not require knowledge of the carrier phase. In addition, NSE has the advantage of being much more robust against frequency offset than coherent MLSE [12], i.e., complex phase and frequency synchronization circuits (e.g., phase–locked loops (PLLs)) can be avoided. However, NSE still requires – up to a constant phase term – knowledge of the channel impulse response. Conventional LMS or RLS algorithms, which may be considered as coherent adaptive algorithms, should not be used for channel identification in this case since they are sensitive to carrier phase variations and are not able to deliver a reliable estimate even for relatively small frequency offsets. Thus, it is necessary to employ robust noncoherent adaptive channel identification algorithms especially tailored for NSE. Although noncoherent linear and nonlinear adaptive equalization schemes have already been proposed in literature [14, 15, 16, 17, 18], the problem of noncoherent adaptive channel identification using noncoherent LMS (NLMS) or RLS (NRLS) algorithms has not been considered so far. In [19] more complex Kalman filters were proposed for noncoherent channel identification. However, Kalman filters require a priori knowledge about the statistical properties of the underlying fading channel, which might be difficult to obtain in mobile applications.

In this letter, we design NLMS and NRLS algorithms which deliver – up to a constant phase term – an estimate of the channel impulse response. Both are very robust against frequency offsets and simulations confirm that their convergence speed is similar to that of their conventional counterparts. For NSE, the so–called *Forney approach* proposed by Colavolpe and Raheli [9, 10, 11] (referred to as CR–NSE) is employed because of its very high performance. Our simulations show that the combination of CR–NSE and the proposed NLMS and NRLS algorithms results in a robust receiver for MDPSK transmission over time–variant ISI channels.

2 Transmission Model and Receiver Structure

2.1 Transmission Model

Fig. 1 shows a block diagram of the discrete–time transmission model. All signals are represented by their complex–valued baseband equivalents. At the transmitter, the MDPSK symbols $a[\cdot] \in \mathcal{A} = \{e^{j2\pi\nu/M} | \nu \in \{0, 1, \ldots, M-1\}\}$ are differentially encoded. The resulting MPSK symbols $b[\cdot] \in \mathcal{A}$ are given by

$$b[k] = a[k]b[k-1], \quad k \in \mathbb{Z}. \tag{1}$$

The complex–valued coefficients of the possibly time–variant combined discrete–time impulse response of transmit filter, channel, and receiver input filter are denoted by $h_l[k]$, $0 \leq l \leq L-1$. L is the length of the impulse response. Θ denotes an unknown, constant, uniformly distributed phase shift introduced by the channel. We assume that the demodulator frequency offset Δf is small and thus, its effect on the discrete–time model can be approximately represented by a multiplicative factor $e^{j2\pi\Delta fTk}$ (T is the symbol interval). Furthermore, the receiver input filter has a square–root Nyquist frequency response[1], i.e., the zero–mean complex Gaussian noise $n[\cdot]$ is white. Due to an appropriate normalization, the variance of $n[\cdot]$ is $\sigma_n^2 = \mathcal{E}\{|n[k]|^2\} = N_0/E_S$, where $\mathcal{E}\{\cdot\}$ denotes expectation. E_S and N_0 are the mean received energy per symbol and the single–sided power spectral density of the underlying passband noise process, respectively.

The discrete–time received signal sampled at times kT at the output of the receiver input filter can be written as

$$r[k] = e^{j\Theta} e^{j2\pi\Delta fTk} \sum_{l=0}^{L-1} h_l[k]b[k-l] + n[k]. \tag{2}$$

2.2 Receiver Structure

In this letter, we exclusively use CR–NSE because of its high performance. Nevertheless, the proposed channel identification schemes can be applied also to other kinds of NSE algorithms, of course. In particular, it can be employed in combination with the NSE scheme recently proposed in [13], which may be viewed as a generalization of *vector tracking* [20] to signals corrupted by ISI.

The accumulated metric $\Lambda[k]$ to be minimized for CR–NSE is given by

$$\Lambda[k] \triangleq \sum_{\nu=0}^{k} \lambda[k-\nu], \tag{3}$$

[1] This also contains the whitened matched filter [1] as a special case.

where

$$\lambda[k] \triangleq |\tilde{y}[k]|^2 + 2\left|\sum_{\nu=1}^{N-1} r[k-\nu]\tilde{y}^*[k-\nu]\right| - 2\left|\sum_{\nu=0}^{N-1} r[k-\nu]\tilde{y}^*[k-\nu]\right| \tag{4}$$

is the branch metric ($(\cdot)^*$ denotes complex conjugation). Here, N, $N \geq 2$, denotes the number of received samples $r[\cdot]$ used for calculation of $\lambda[k]$. Note that the original branch metric $\lambda'[k]$ in [11] is $\lambda'[k] = -\frac{1}{2}\lambda[k]$. The modification used here has no influence on the performance of the resulting NSE scheme, however, it facilitates the derivation of the noncoherent channel identification algorithms (cf. Section 3). $\tilde{y}[k]$ is given by

$$\tilde{y}[k] \triangleq \sum_{l=0}^{L-1} \hat{h}_l[k]\tilde{b}[k-l], \tag{5}$$

where $\hat{h}_l[k]$, $0 \leq l \leq L-1$, are the coefficients of the estimated channel impulse response. For $0 \leq l \leq K$ (K, $0 \leq K \leq N+L-3$, denotes the number of symbols used for trellis definition), the hypothetical symbols $\tilde{b}[k-l] \in \mathcal{A}$ are defined by the transition $t[k] \triangleq (\tilde{b}[k], \tilde{b}[k-1], \ldots, \tilde{b}[k-K])$ from state $S[k] \triangleq (\tilde{b}[k-1], \tilde{b}[k-2], \ldots, \tilde{b}[k-K])$ to state $S[k+1]$ in the underlying trellis diagram. The number of states is $Z = M^K$. For $l \geq K+1$, the symbols $\tilde{b}[k-l]$ are taken from the surviving path terminating in state $S[k]$, i.e., decision–feedback sequence estimation (DFSE) [21] is employed to limit complexity of CR–NSE [11]. Note that this is necessary for a fair comparison with coherent MLSE since, in general, full–state CR–NSE requires a larger number of states than the coherent full–state Viterbi algorithm [22].

Introducing a decision delay of k_0 time steps the estimated MPSK symbol $\hat{b}[k-k_0]$ is taken from the surviving path with minimum accumulated metric $\Lambda[k]$. For coherent MLSE usually a decision delay $k_0 = 5 \cdot (L-1)$ ($L-1$ is the memory length of the channel) is employed [7]. We use the same decision delay for CR–NSE since our simulations have confirmed that performance cannot be improved by a larger value for k_0. As typical for noncoherent detection schemes, the estimated MPSK symbols may be shifted by a constant phase compared to the transmitted symbols. Thus, differential encoding is necessary and the estimated MDPSK symbols are obtained from $\hat{a}[k-k_0] = \hat{b}[k-k_0]\hat{b}^*[k-k_0-1]$.

Like conventional LMS and RLS algorithms, the noncoherent adaptive algorithms of Section 3 require knowledge of the transmitted symbol sequence. Thus, the estimated transmitted symbols are also delivered to the channel estimator. Especially, for fast time–variant channels the decision delay k_0 may be too large for reliable tracking of the channel impulse response. Therefore, like in the coherent case [4], a smaller decision delay $k_1 \leq k_0$ may be used for channel estimation (cf. Fig. 1). Since the estimated transmitted symbols are the less reliable the smaller k_1 is chosen, while the tracking properties are improved for smaller values of k_1, there is a trade–off and k_1 has to be optimized for the particular channel. We also would like

to mention that the decision delay could be avoided by application of *per–survivor processing* [23] at the expense of a higher receiver complexity.

3 Noncoherent Adaptive Channel Identification

In this section, an NLMS and an NRLS algorithm for identification and tracking of the channel impulse response are derived. Furthermore, their performance under frequency offset and their convergence behaviour are investigated.

3.1 NLMS Algorithm

For derivation of the NLMS algorithm, for simplicity, the decision delay k_1 is not taken into account. A gradient adaptation algorithm is obtained if the vector $\hat{\boldsymbol{h}}[k] \triangleq [\hat{h}_0[k]\ \hat{h}_1[k]\ \ldots\ \hat{h}_{L-1}[k]]^H$ ($[\cdot]^H$ denotes Hermitian transposition) of (complex–conjugated) coefficients of the estimated impulse response is updated according to the recursive relation [7, 8]

$$\hat{\boldsymbol{h}}[k+1] = \hat{\boldsymbol{h}}[k] - \delta_{\mathrm{LMS}} \frac{\partial}{\partial \hat{\boldsymbol{h}}^*[k]} J(\hat{\boldsymbol{h}}[k]), \tag{6}$$

where δ_{LMS} denotes the adaptation step size and $J(\hat{\boldsymbol{h}}[k])$ is an appropriate cost function.

For the conventional LMS algorithm $J_{\mathrm{CLMS}}(\hat{\boldsymbol{h}}[k]) \triangleq |r[k] - \hat{\boldsymbol{h}}^H[k]\boldsymbol{b}[k]|^2$ ($\boldsymbol{b}[k] \triangleq [b[k]\ b[k-1]\ \ldots\ b[k-L+1]]^T$; $[\cdot]^T$ denotes transposition) is used as cost function, i.e., $J_{\mathrm{CLMS}}(\hat{\boldsymbol{h}}[k])$ is minimized recursively with respect to $\hat{\boldsymbol{h}}[k]$ provided that $\boldsymbol{b}[k]$ is known. On the other hand, for coherent MLSE $J_{\mathrm{CLMS}}[k]$ is used as branch metric and minimized with respect to $\boldsymbol{b}[k]$ provided that the impulse response $\hat{\boldsymbol{h}}[k]$ is known.

This brief review of the coherent receiver suggests to use the branch metric (cf. Eq. (4)) of CR–NSE as (noncoherent) cost function $J_{\mathrm{NLMS}}(\hat{\boldsymbol{h}}[k])$ for the NLMS algorithm. Thus, we define

$$J_{\mathrm{NLMS}}(\hat{\boldsymbol{h}}[k]) \triangleq |y[k]|^2 + 2\left|\sum_{\nu=1}^{N_{\mathrm{NLMS}}-1} r[k-\nu]y^*[k-\nu]\right| - 2\left|\sum_{\nu=0}^{N_{\mathrm{NLMS}}-1} r[k-\nu]y^*[k-\nu]\right|, \tag{7}$$

with

$$y[k] \triangleq \hat{\boldsymbol{h}}^H[k]\boldsymbol{b}[k]. \tag{8}$$

N_{NLMS}, $N_{\mathrm{NLMS}} \geq 2$, denotes the number of received signal samples $r[\cdot]$ used for calculation of $J_{\mathrm{NLMS}}(\hat{\boldsymbol{h}}[k])$. Note that N_{NLMS} does not have to coincide with N used for CR–NSE. Using similar methods as proposed in [17] for derivation of filter adaptation for noncoherent decision–feedback equalization (NDFE), the NLMS algorithm for identification of the channel impulse

response can be derived from $J_{\mathrm{NLMS}}(\hat{\boldsymbol{h}}[k])$. The resulting recursive relation for updating $\hat{\boldsymbol{h}}[k]$ is

$$\hat{\boldsymbol{h}}[k+1] = \hat{\boldsymbol{h}}[k] + \delta_{\mathrm{LMS}} e^*_{\mathrm{NLMS}}[k]\boldsymbol{b}[k], \tag{9}$$

where the definitions

$$e_{\mathrm{NLMS}}[k] \triangleq \frac{q^*_{N_{\mathrm{NLMS}}}[k]}{|q_{N_{\mathrm{NLMS}}}[k]|} r[k] - y[k], \tag{10}$$

$$q_{N_{\mathrm{NLMS}}}[k] \triangleq \sum_{\nu=0}^{N_{\mathrm{NLMS}}-1} r[k-\nu]y^*[k-\nu] \tag{11}$$

are valid. A comparison of the NLMS with the conventional LMS algorithm shows that the only difference is the additional factor $q^*_{N_{\mathrm{NLMS}}}[k]/|q_{N_{\mathrm{NLMS}}}[k]|$ in Eq. (10). This factor is the maximum–likelihood (ML) estimate of the phase difference between $y[\cdot]$ and $r[\cdot]$ [11]. Thus, the proposed NLMS algorithm can be interpreted as conventional LMS algorithm with incorporated ML phase estimation.

If $\hat{\boldsymbol{h}}[0]$ is initialized with the all zero vector, $q_{N_{\mathrm{NLMS}}}[0] = 0$ follows and $q_{N_{\mathrm{NLMS}}}[0]/|q_{N_{\mathrm{NLMS}}}[0]|$ is not defined. In this case, we suggest to use the initialization $q_{N_{\mathrm{NLMS}}}[0]/|q_{N_{\mathrm{NLMS}}}[0]| = 1$ in Eq. (10).

3.2 NRLS Algorithm

Besides the simple conventional LMS, the faster converging conventional RLS algorithm [7, 8] is frequently used for channel estimation. Thus, for fast adaptation a noncoherent RLS (NRLS) algorithm is also desirable.

Considering the analogy between the conventional LMS and the conventional RLS algorithm [7, 8], and employing the same approach as in [17] for NDFE, an NRLS algorithm for noncoherent channel estimation can be obtained easily. The estimated impulse response may be calculated recursively using the following equations:

$$\boldsymbol{l}[k] = \frac{\boldsymbol{P}[k-1]\boldsymbol{b}[k]}{w + \boldsymbol{b}^H[k]\boldsymbol{P}[k-1]\boldsymbol{b}[k]}, \tag{12}$$

$$\xi_{\mathrm{NRLS}}[k] = \frac{(q_{N_{\mathrm{NRLS}}}[k-1])^*}{|q_{N_{\mathrm{NRLS}}}[k-1]|} r[k] - \hat{\boldsymbol{h}}^H[k-1]\boldsymbol{b}[k], \tag{13}$$

$$\hat{\boldsymbol{h}}[k] = \hat{\boldsymbol{h}}[k-1] + \boldsymbol{l}[k]\xi^*_{\mathrm{NRLS}}[k], \tag{14}$$

$$\boldsymbol{P}[k] = w^{-1}\boldsymbol{P}[k-1] - w^{-1}\boldsymbol{l}[k]\boldsymbol{b}^H[k]\boldsymbol{P}[k-1], \tag{15}$$

where w, $0 < w \leq 1$, is the forgetting factor of the algorithm. N_{NRLS}, $N_{\mathrm{NRLS}} > 2$, has a similar meaning as N_{NLMS} for the NLMS algorithm. For initialization of $\boldsymbol{P}[0]$, we propose

$$\boldsymbol{P}[0] = \delta^{-1}_{\mathrm{RLS}}\boldsymbol{I}_{L\times L}, \tag{16}$$

where δ_{RLS} is a small positive constant (typical value: 0.001) and $\boldsymbol{I}_{L\times L}$ denotes the $L \times L$ identity matrix. If $\hat{\boldsymbol{h}}[k-1]$ is initialized with the all zero vector, $q_{N_{\mathrm{NRLS}}}[0]/|q_{N_{\mathrm{NRLS}}}[0]| = 1$ is used at $k = 1$.

3.3 Influence of Phase Shift and Frequency Offset

In this section, we focus on the NLMS algorithm, however, the results obtained can be extended easily to the NRLS algorithm.

First, we investigate the influence of phase shift and frequency offset on the conventional LMS algorithm. For this purpose, the corresponding error signal $e_{\mathrm{CLMS}}[k] \triangleq r[k] - y[k]$ [8] may be considered. For simplicity, here the channel noise is neglected. If $r[k]$ and $y[k]$ given by Eqs. (2) and (8), respectively, are applied,

$$e_{\mathrm{CLMS}}[k] = \left(\mathrm{e}^{j\Theta}\mathrm{e}^{j2\pi\Delta fTk}\boldsymbol{h}^H[k] - \hat{\boldsymbol{h}}^H[k]\right)\boldsymbol{b}[k] \tag{17}$$

is obtained, where the definition $\boldsymbol{h}[k] \triangleq [h_0[k]\ h_1[k]\ \ldots\ h_{L-1}[k]]^T$ is used. Eq. (17) clearly shows that the error $e_{\mathrm{CLMS}}[k]$ depends on both phase shift Θ and frequency offset Δf. Thus, in order to minimize $e_{\mathrm{CLMS}}[k]$, the conventional LMS algorithm has to estimate not only the channel impulse response $\boldsymbol{h}[k]$ but implicitly also Θ and more importantly, it has to track the frequency offset. Our simulations in Section 3.4 show that, even for relatively small frequency offsets, the conventional LMS algorithm is not able to perform this difficult task, i.e., an additional frequency offset compensation unit is necessary.

The error signal $e_{\mathrm{NLMS}}[k]$ (cf. Eq. (10)) of the NLMS algorithm may be rewritten to

$$e_{\mathrm{NLMS}}[k] = \left(\frac{\left(\sum_{\nu=0}^{N_{\mathrm{NLMS}}-1}\mathrm{e}^{-j2\pi\Delta fT\nu}\boldsymbol{h}^H[k-\nu]\boldsymbol{b}[k-\nu]\boldsymbol{b}^H[k-\nu]\hat{\boldsymbol{h}}[k-\nu]\right)^*}{\left|\sum_{\nu=0}^{N_{\mathrm{NLMS}}-1}\mathrm{e}^{-j2\pi\Delta fT\nu}\boldsymbol{h}^H[k-\nu]\boldsymbol{b}[k-\nu]\boldsymbol{b}^H[k-\nu]\hat{\boldsymbol{h}}[k-\nu]\right|}\boldsymbol{h}^H[k] - \hat{\boldsymbol{h}}^H[k]\right)\boldsymbol{b}[k]. \tag{18}$$

Eq. (18) demonstrates that $e_{\mathrm{NLMS}}[k]$ is independent of Θ which underlines the noncoherent character of the proposed NLMS algorithm. On the other hand, the influence of the frequency offset is limited to the factor $\left(\sum_{\nu=0}^{N_{\mathrm{NLMS}}-1}\mathrm{e}^{-j2\pi\Delta fT\nu}\boldsymbol{h}^H[k-\nu]\boldsymbol{b}[k-\nu]\boldsymbol{b}^H[k-\nu]\hat{\boldsymbol{h}}[k-\nu]\right)^* / \left|\sum_{\nu=0}^{N_{\mathrm{NLMS}}-1}\mathrm{e}^{-j2\pi\Delta fT\nu}\boldsymbol{h}^H[k-\nu]\boldsymbol{b}[k-\nu]\boldsymbol{b}^H[k-\nu]\hat{\boldsymbol{h}}[k-\nu]\right|$, where the frequency offset appears only in terms of the form $\mathrm{e}^{-j2\pi\Delta fT\nu}$, $0 \le \nu \le N_{\mathrm{NLMS}} - 1$. Thus, it can be expected that small frequency offsets do not influence the estimated impulse response $\hat{\boldsymbol{h}}[k]$ as long as N_{NLMS} is not chosen too large.

3.4 Convergence of Adaptive Algorithms

A stability and convergence analysis of the proposed noncoherent adaptive algorithms is very difficult if not impossible due to their nonlinear character. Therefore, we have to restrict ourselves to computer simulations. As far as stability is concerned, our simulations showed that the step size parameter δ_{LMS} of the NLMS algorithm has to fulfill similar conditions like the step size parameter of the conventional LMS algorithm [8]. Furthermore, the NRLS algorithm showed no instabilities for the same range of w as the conventional RLS algorithm.

In the following, the convergence speed of the NLMS algorithm will be compared with that of the conventional LMS algorithm. For this, a constant ISI channel with $\boldsymbol{h}[k] = 1/\sqrt{19} \cdot [1\ 2\ 3\ 2\ 1]^T$ ($L = 5$), $\forall\, k$, and a training sequence of QDPSK symbols (i.e., $M = 4$) are used. The learning curves [8] are averaged over 1000 adaptation processes and $10\log_{10}(E_b/N_0) = 15$ dB ($E_b = E_S/2$ denotes the mean received energy per bit) is valid.

Figs. 2a) and b) show the learning curves for the proposed NLMS and the conventional LMS algorithm for normalized frequency offsets of $\Delta fT = 0$ and $\Delta fT = 0.02$, respectively. The step size parameter $\delta_{\mathrm{LMS}} = 0.05$ is used in all cases. For the NLMS algorithm $J'_{\mathrm{LMS}}[k]$ is defined as $J'_{\mathrm{LMS}}[k] \triangleq \mathcal{E}\{|e_{\mathrm{NLMS}}[k]|^2\}$, whereas for the conventional LMS algorithm the usual definition (cf. e.g. [8]) is employed. Fig. 2a) shows that, in the absence of frequency offset, the NLMS algorithm has a similar convergence speed and causes a similar steady–state error like the conventional LMS algorithm. In addition, the performance of the NLMS algorithm is almost independent of N_{NLMS}. On the other hand, for $\Delta fT = 0.02$, Fig. 2b) clearly illustrates that the conventional LMS algorithm does not converge to a reasonable solution; it is not able to compensate the frequency offset. The proposed NLMS algorithm, however, converges in all cases. The frequency offset only increases the steady–state error, while the convergence speed is hardly influenced. Since for $\Delta fT > 0$ the steady–state error is higher for larger N_{NLMS}, $N_{\mathrm{NLMS}} = 2$ will be used exclusively in our simulations presented in Section 4.

Similar results can be obtained for the NRLS algorithm, i.e., $N_{\mathrm{NRLS}} = 2$ turns out to be the best choice and its convergence speed is comparable with that of the conventional RLS algorithm.

4 Simulation Results

For all simulations presented in this section a burst transmission is assumed. Each burst contains a preamble of 14 QDPSK training symbols and 160 QDPSK data symbols. The entire training sequence (TS) is used for least–squares (LS) estimation [8] of the channel impulse response as it is customary in mobile communications [24, 5]. Note that the LS approach for initial impulse response estimation is suitable for both coherent and noncoherent sequence estimation since it does not degrade severely under carrier phase variations. In time–variant

environments, the initial estimate delivered by the LS estimator may be considered as the *mean* channel impulse response during the TS. Hence, the adaptive algorithms start in the middle of the TS. Since the NLMS (NRLS) algorithm is more robust against frequency offset for smaller N_{NLMS} (N_{NRLS}), in the following, we will use exclusively $N_{\mathrm{NLMS}} = 2$ ($N_{\mathrm{NRLS}} = 2$). It is worth mentioning that the training sequence is also used for initialization and termination of the trellis of coherent MLSE and CR–NSE.

The impulse response length is $L = 3$ for both examples presented below. In the coherent case, a full–state Viterbi algorithm [1, 22] is employed, i.e., the number of states is $Z = 16$. For CR–NSE the same number of states is used, i.e., DFSE [21, 11] is applied. The decision delay k_1 for the adaptive algorithms is $k_1 = 2$ in all cases since this value yields the best results for the time–variant channels used here.

In our first example, a frequency–selective time–variant three–tap Rayleigh fading channel is employed. All three taps fade independently according to Jakes Model [25]. The normalized fading bandwidth of all taps is $B_f T = 0.001$, where B_f denotes the single–sided bandwidth of the underlying continuous–time fading process. The second and the third tap are attenuated by 3 dB and 6 dB in comparison to the first tap, respectively. Fig. 3 shows BER vs. $10\log_{10}(E_b/N_0)$ for coherent MLSE combined with the conventional LMS algorithm and CR–NSE combined with the NLMS algorithm. $\delta_{\mathrm{LMS}} = 0.1$ is used for all curves since this value yields the best performance for LMS and NLMS algorithm, respectively. It can be observed that the noncoherent receiver approaches the coherent receiver for zero frequency offset as N increases. In addition, a frequency offset of $\Delta f T = 0.01$ causes only a small loss in power efficiency if the proposed noncoherent receiver is employed.

In Fig. 4, we compare coherent MLSE combined with the conventional RLS algorithm and CR–NSE combined with the NRLS algorithm. Again a three–tap Rayleigh fading channel is employed, however, now $B_f T = 0.0015$ is used and all taps have equal power. A forgetting factor of $w = 0.88$ was found to be optimum in all cases. Again, for $\Delta f T = 0$ the noncoherent receiver approaches the coherent one and it yields also a good performance for $\Delta f T = 0.01$.

From the above examples it can be seen that for the proposed noncoherent receiver there is a trade–off between power efficiency for $\Delta f T = 0$ and robustness against frequency offset. Although power efficiency for zero frequency offset increases with increasing N, the sensitivity to carrier phase variations increases, too. Thus, in a practical application the proper choice of N depends on the maximum expected frequency offset in the system.

5 Conclusions

Noncoherent adaptive channel identification has been introduced in this paper. NLMS and NRLS algorithms have been derived and their robustness against carrier phase variations

was demonstrated. It has been shown that in the absence of frequency offset the proposed adaptive algorithms have a similar performance as conventional LMS and RLS algorithms. On the other hand, the novel noncoherent algorithms also converge under frequency offset, whereas their conventional counterparts diverge. It has also been shown that the optimum value for the block size N_{NLMS} (N_{NRLS}) of the NLMS (NRLS) algorithm is 2.

Moreover, it was confirmed by computer simulations that the combination of CR–NSE and noncoherent adaptive channel identification provides a robust receiver, which is insensitive to carrier phase variations, i.e., complex synchronization units necessary for coherent adaptive MLSE receivers can be avoided. In the absence of phase variations, the loss in power efficiency of the noncoherent receiver in comparison to a corresponding coherent receiver is small.

Acknowledgement

The authors would like to thank TCMC (Technology Centre for Mobile Communication), Philips Semiconductors, Germany, for supporting this work. Furthermore, they are grateful to G. Colavolpe for providing a preprint of reference [11]. They are also in debt of Prof. J. B. Huber for helpful discussions and his encouragement throughout the development of this paper. Finally, the authors wish to acknowledge the helpful comments of the reviewers and the Associate Editor.

References

[1] G.D. Forney, Jr. Maximum–Likelihood Sequence Estimation of Digital Sequences in the Presence of Intersymbol Interference. *IEEE Trans. on Inf. Theory*, IT-18:363–378, 1972.

[2] G. Ungerböck. Adaptive maximum–likelihood receiver for carrier–modulated data–transmission systems. *IEEE Trans. on Commun.*, COM-22:624–636, 1974.

[3] Jr. F. R. Magee and J. G. Proakis. Adaptive maximum–likelihood sequence estimation for digital signaling in the presence of intersymbol interference. *IEEE Trans. on Inf. Theory*, IT-19:120–124, January 1973.

[4] S.U.H. Qureshi and E.E. Newhall. An Adaptive Receiver for Data Transmission over Time-Dispersive Channels. *IEEE Trans. on Inf. Theory*, IT-19:448–457, July 1973.

[5] J. G. Proakis. Adaptive Equalization for TDMA Digital Mobile Radio. *IEEE Trans. on Veh. Tech.*, 40:333–341, May 1991.

[6] R. d'Avella, L. Moreno, and M. Sant'Agostino. An Adaptive MLSE Receiver for TDMA Digital Mobile Radio. *IEEE Journal on Selected Areas in Communications*, 7:122–129, January 1989.

[7] J.G. Proakis. *Digital Communications*. McGraw–Hill, New York, Third Edition, 1995.

[8] S. Haykin. *Adaptive Filter Theory*. Prentice-Hall, Upper Saddle River, New Jersey, Third Edition, 1996.

[9] R. Raheli and G. Colavolpe. Noncoherent Sequence Detection: a New Perspective in Receiver Design. In *Proceedings of the International Conference on Telecommunications (ICT'98)*, pages 265–269, Porto Carras, June 1998.

[10] G. Colavolpe and R. Raheli. Noncoherent Sequence Detection of Continuous Phase Modulations. In *Proceedings of Globecom'98*, pages 556–561, Sydney, November 1998.

[11] G. Colavolpe and R. Raheli. Noncoherent Sequence Detection. *IEEE Trans. on Commun.*, COM-47:1376–1385, September 1999.

[12] W. Gerstacker, R. Schober, and J. Huber. Noncoherent Equalization Algorithms Based on Sequence Estimation. In *Proceedings of Globecom'98*, pages 3485–3490, Sydney, November 1998.

[13] R. Schober and W. H. Gerstacker. Metric for noncoherent sequence estimation. *Electronics Letters*, 35(25):2178–2179, November 1999.

[14] P. Sehier and G. Kawas Kaleh. Adaptive equaliser for differentially coherent receiver. *IEE Proceedings-I*, 137:9–12, February 1990.

[15] A. Masoomzadeh-Fard and S. Pasupathy. Nonlinear Equalization of Multipath Fading Channels with Noncoherent Demodulation. *IEEE Journal on Selected Areas in Communications*, SAC-14:512–520, April 1996.

[16] R. Schober, W. H. Gerstacker, and J. B. Huber. Adaptive Linear Equalization Combined with Noncoherent Detection of MDPSK Signals. *IEEE Trans. on Commun.*, COM-48:733–738, May 2000.

[17] R. Schober, W. H. Gerstacker, and J. B. Huber. Adaptive Noncoherent DFE for MDPSK Signals Transmitted Over ISI Channels. *IEEE Trans. on Commun.*, COM-48:1128–1140, July 2000.

[18] R. Schober, W. H. Gerstacker, and J. B. Huber. Adaptive Noncoherent Linear Minimum ISI Equalization. *In Revision: IEEE Trans. on Signal Processing*, June 1999.

[19] Q. Dai and E. Shwedyk. Detection of Bandlimited Signals Over Frequency Selective Rayleigh Fading Channels. *IEEE Trans. on Commun.*, COM-42:941–950, Feb.-Apr. 1994.

[20] A. N. D'Andrea, U. Mengali, and G. M. Vitetta. Approximate ML Decoding of Coded PSK with No Explicit Carrier Phase Reference. *IEEE Trans. on Commun.*, COM-42:1033–1039, Feb.-Apr. 1994.

[21] A. Duel-Hallen and A. C. Heegard. Delayed Decision–Feedback Sequence Estimation. *IEEE Trans. on Commun.*, COM-37:428–436, 1989.

[22] G.D. Forney, Jr. The Viterbi Algorithm. *IEEE Proceedings*, 61:268–278, 1973.

[23] R. Raheli, A. Polydoros, and C.-K. Tzou. Per-Survivor Processing: A General Approach to MLSE in Uncertain Environments. *IEEE Trans. on Commun.*, COM-43:354–364, February/March/April 1995.

[24] S.N. Crozier, D.D. Falconer, and S.A. Mahmoud. Least sum of squared errors (LSSE) channel estimation. *IEE Proceedings-F*, 138:371–378, August 1991.

[25] Ed. W. C. Jakes, Jr. *Microwave Mobile Communications.* Prentice–Hall, New Jersey, 1974.

Figure Captions:

Figure 1: Block diagram of the discrete–time transmission and receiver model under consideration.

Figure 2: Learning curves for NLMS and conventional LMS algorithm. a) $\Delta fT = 0$, and b) $\Delta fT = 0.02$. For both figures $\boldsymbol{h}[k] = 1/\sqrt{19} \cdot [1\ 2\ 3\ 2\ 1]^T$, $10\log_{10}(E_b/N_0) = 15$ dB, and $\delta_{\mathrm{LMS}} = 0.05$ are valid.

Figure 3: BER vs. $10\log_{10}(E_b/N_0)$ for NSE combined with NLMS algorithm and coherent MLSE combined with conventional LMS algorithm. A three–tap Rayleigh fading channel ($B_fT = 0.001$) is used. All taps fade independently and the second and the third tap are attenuated by 3 dB and 6 dB, respectively, in comparison to the first tap.

Figure 4: BER vs. $10\log_{10}(E_b/N_0)$ for NSE combined with NRLS algorithm and coherent MLSE combined with conventional RLS algorithm. A three–tap Rayleigh fading channel ($B_fT = 0.0015$) is used. All taps fade independently and have equal mean power.

Figures:

Figure 1:

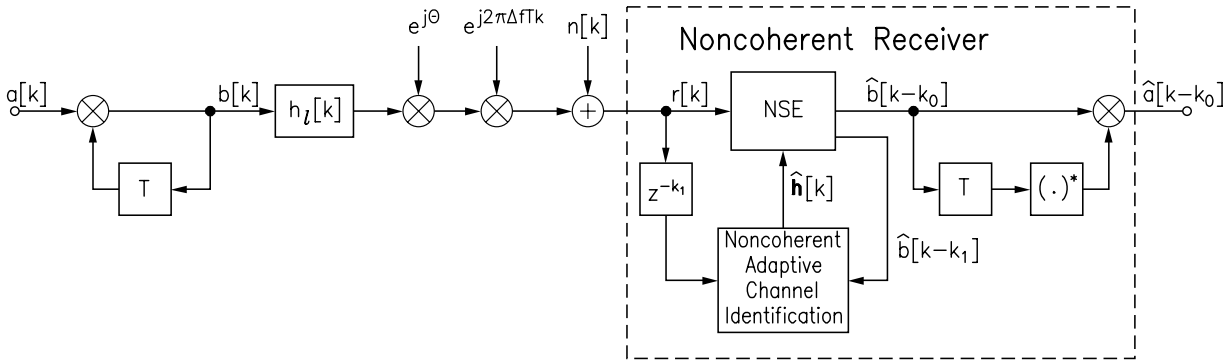

Figure 2:

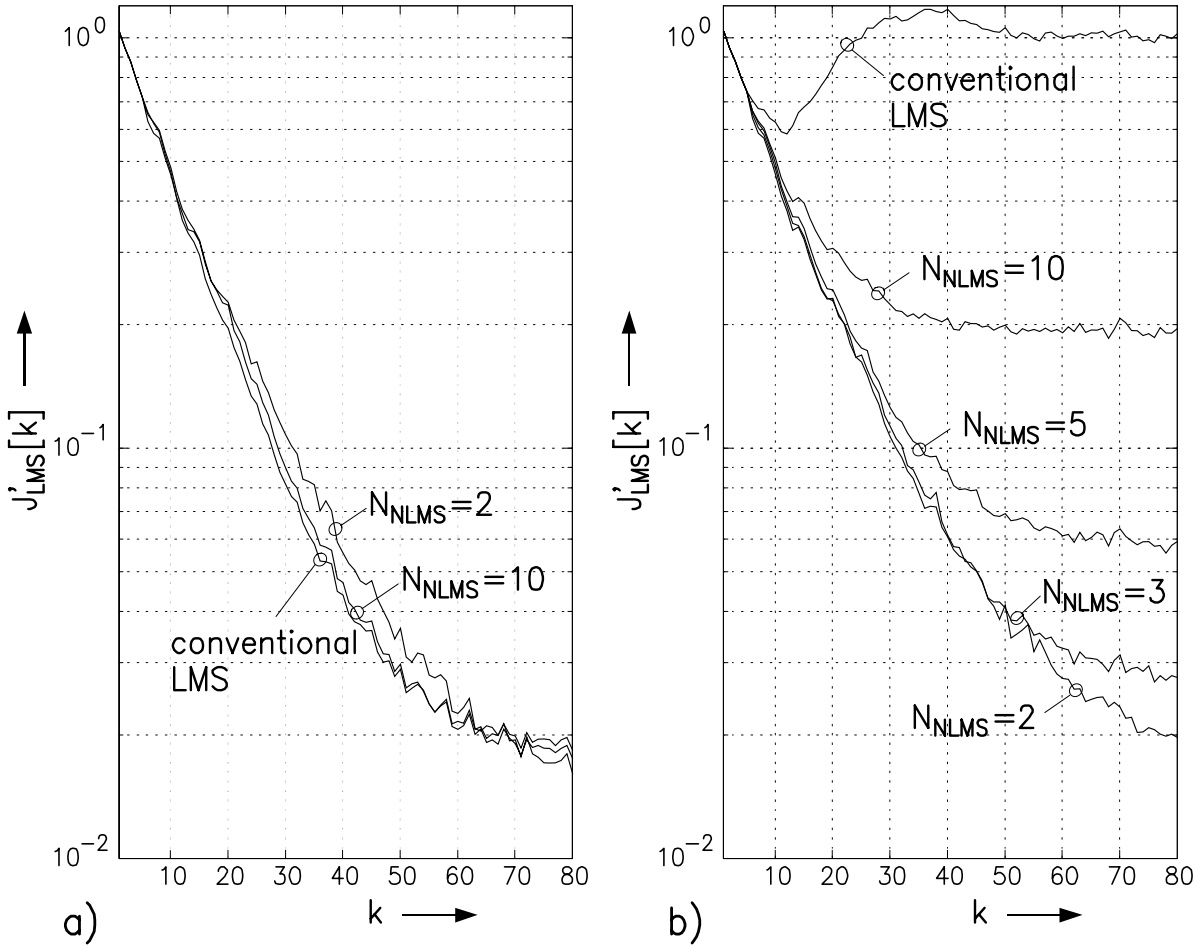
10^0
10^{-1}
10^{-2}
$J'_{LMS}[k]$
$N_{NLMS}=2$
$N_{NLMS}=10$
conventional
LMS
10 20 30 40 50 60 70 80
k
a)
10^0
10^{-1}
10^{-2}
$J'_{LMS}[k]$
conventional
LMS
$N_{NLMS}=10$
$N_{NLMS}=5$
$N_{NLMS}=3$
$N_{NLMS}=2$
10 20 30 40 50 60 70 80
k
b)

Figure 3:

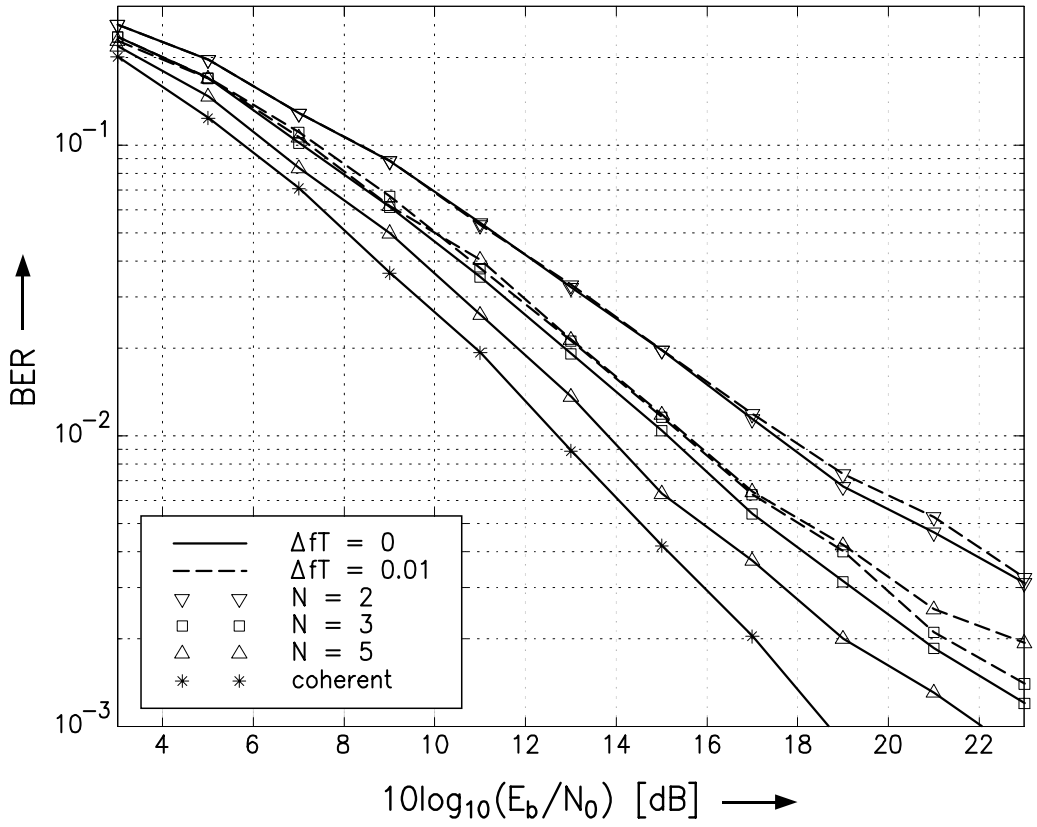
BER
10^{-1}
10^{-2}
10^{-3}
4
6
8
10
12
14
16
18
20
22
$10\log_{10}(E_b/N_0)$ [dB]
ΔfT = 0
ΔfT = 0.01
N = 2
N = 3
N = 5
coherent

Figure 4:

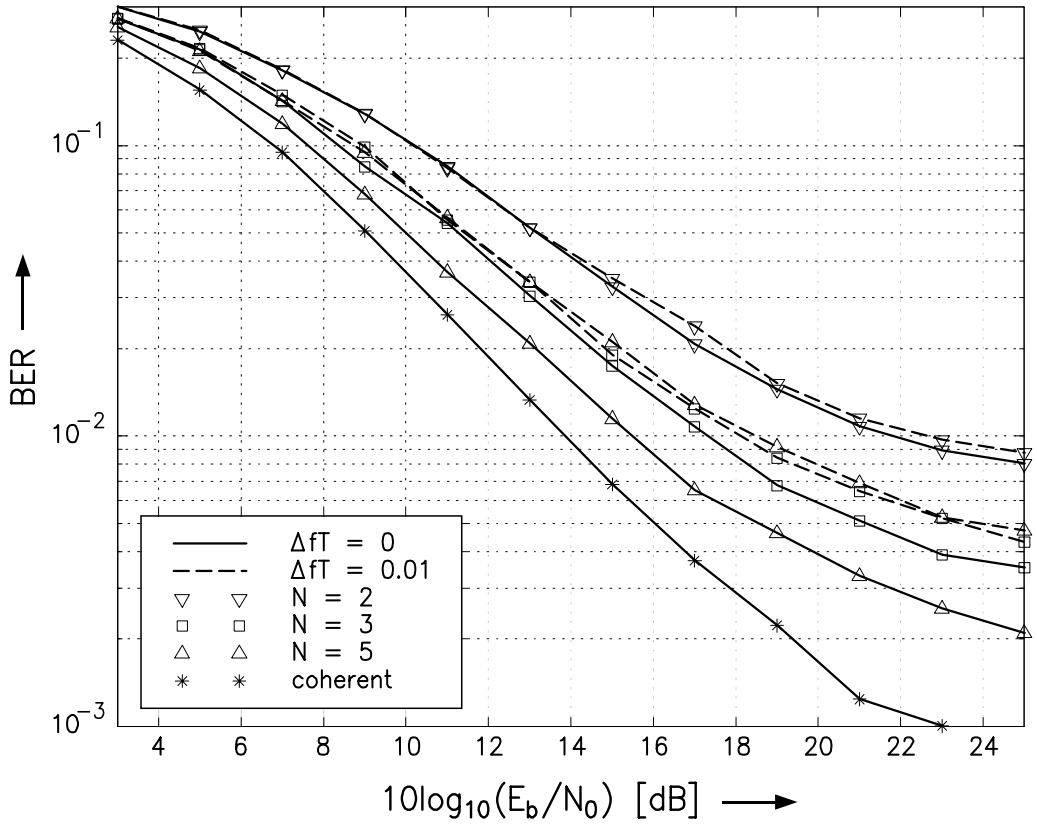
BER
10^{-1}
10^{-2}
10^{-3}
4
6
8
10
12
14
16
18
20
22
24
$10\log_{10}(E_b/N_0)$ [dB]
ΔfT = 0
ΔfT = 0.01
N = 2
N = 3
N = 5
coherent